Wave Motion 48 (2011) 814–823

Contents lists available at ScienceDirect

Wave Motion

journal homepage: www.elsevier.com/locate/wavemoti

Stability of exothermic autocatalytic fronts with regard to buoyancy-driven instabilities in presence of heat losses

T. Gérard, A. De Wit *

Nonlinear Physical Chemistry Unit and Centre for Nonlinear Phenomena and Complex Systems, CP 231, Faculté des Sciences, Campus Plaine, Université Libre de Bruxelles (ULB), 1050 Brussels, Belgium

ARTICLE INFO

Article history:
Received 28 February 2011
Received in revised form 25 April 2011
Accepted 28 April 2011
Available online 7 May 2011

Keywords:
Heat losses
Autocatalytic front
Rayleigh-Taylor
Convection
Exothermic front
Fingering

ABSTRACT

Across traveling autocatalytic fronts, density differences due to composition and temperature changes can lead to buoyancy-driven hydrodynamic instabilities deforming the front by convective motions. We study here the influence of heat losses through the walls of the reactor on the stability of such exothermic fronts in the gravity field. The stability domain is computed numerically in a parameter space spanned by the solutal R_c and thermal R_T Rayleigh numbers of the problem for various values of the Newton's coefficient α quantifying the intensity of heat losses.

1. Introduction

Traveling fronts, whereby products of reaction invade progressively fresh reactants in space and time at a constant speed, result from the coupling between autocatalytic reactions and diffusion and have largely been studied both experimentally and theoretically [1–3]. In absence of gels ensuring that diffusion is the only transport phenomenon taking place, convection can deform such fronts. Indeed, composition and temperature changes across the front can induce a density jump susceptible to drive buoyancy-driven convective motions in the gravity field. Explicitly, the density difference across the front $\Delta\rho = \rho_p - \rho_r$, i.e. the difference between the density of the products ρ_p and that of the reactants ρ_r is a combination of a solutal contribution $\Delta\rho_s$ due to the difference in molar volume of the products compared to the reactants and a thermal part $\Delta\rho_T$ due to the exo- or endothermicity of the reaction [3–6]. While $\Delta\rho_s$ can have either sign, the thermal contribution $\Delta\rho_T$ is always negative because no endothermic autocatalytic reaction is known and heat produced in the reaction decreases the density of products.

If the two contributions, $\Delta\rho_s$ and $\Delta\rho_T$, have the same negative sign, the system is in the so-called cooperative regime [6] as solutal and thermal effects act in the same way to decrease the density behind the front. In this case, the reaction leads thus to hot and solute lighter products compared to the reactants that are at room temperature. When the front is traveling upwards in the gravity field, a simple Rayleigh–Taylor instability can occur as denser reactants overlie then less dense products. The related stability and nonlinear dynamics have been extensively studied theoretically and experimentally on the iodate–arsenous acid reaction [3,7–18]. For such cooperative systems, the descending fronts which are in a stable density stratification can however also be unstable because of differential diffusion effects between heat and mass [6,19–21]. On the contrary, if $\Delta\rho_T<0$ but $\Delta\rho_s>0$, the products are hotter but solute–denser. This case is called antagonist as the heat decreases the density of the solution while the change of molar volume increases it. Because of those opposite effects, multicomponent convection and double diffusive instabilities can occur [4–6,20–22] as studied on chlorite–tetrathionate [23–28] reaction fronts for instance.

* Corresponding author.
E-mail address: adewit@ulb.ac.be (A. De Wit).

0165-2125/$ – see front matter © 2011 Elsevier B.V. All rights reserved.
doi:10.1016/j.wavemoti.2011.04.018

A classification of the stability of autocatalytic fronts with regard to Rayleigh–Taylor (RT) and double-diffusive (DD) instabilities has been performed for both cases in isolated systems [6] for different ratios of diffusivity between heat and mass. The larger this ratio, the larger the instability domain of the fronts in a parameter space spanned by the solutal R_c and thermal R_T Rayleigh numbers of the problem. Interestingly, the chemical reaction is able to destabilize a much larger domain than the one obtained for simple linear density profiles in non-reactive systems [21].

Recently, interest has arisen to understand the influence of heat losses through the walls of the reactor on the stability and dynamics of such convectively unstable fronts. Indeed, experimentally, the buoyancy-driven instabilities of autocatalytic fronts are studied in Hele-Shaw cells, quasi-two dimensional reactors made of two glass or plexyglass plates separated by a thin gap where the reaction occurs [14,16,27]. One advantage of this system is the simplicity of recording the pattern's dynamics through the glasses. However, such Hele-Shaw cells cannot be considered as isolated systems because the glass walls dissipate part of the heat out of the system as observed experimentally by magnetic resonance imaging (MRI) [30], infrared camera [28], interferometry [29] or simply a local measurement via a thermocouple [31]. Such heat losses affect directly the temperature profile across the reaction zone as this profile is effectively a pulse in presence of heat losses rather than a front such as for isolated reactors. As a consequence, the thermal contribution to the density of the solution is modified, which has a direct influence on the stability of fronts [32] and on their nonlinear dynamics [32,33].

D'Hernoncourt et al. have started studying theoretically the influence of such heat losses on the dynamics of autocatalytic fronts by linear stability analysis and nonlinear simulations of reaction–diffusion–convection models focusing on the case of cooperative fronts [32,33]. They have shown that heat losses generate non-monotonic density profiles susceptible to destabilize descending fronts otherwise stable in isolated systems [32]. Moreover, the nonlinear dynamics of ascending fronts is then characterized by the presence of four convection rolls per finger instead of two in insulated systems [16], which increases significantly tip splitting phenomena [32,33]. In other situations too, non-monotonic profiles can be observed and modify the stability of interfaces separating fluids [34]. For instance, Yortos et al. [35,36] analyzed non-monotonic mobility profiles during two-phase flow in porous media of water and oil. Loggia et al. [37] also showed the importance of non-monotonic profiles during miscible displacements involving both viscosity and density changes. As last example, non-monotonic density profiles are also observed around simple acid–base reaction fronts [38,39]. In each of these cases, these non-monotonic profiles modify the stability of the interface between solutions.

In this context, the present article aims at complementing the analysis of the influence of heat losses on buoyancy-driven instabilities of autocatalytic fronts by performing a detailed linear stability analysis of the various possible instability scenarios for both cooperative and antagonistic reactions. To do so, we will determine the stability domain of the fronts in a parameter space spanned by the solutal R_c and thermal R_T Rayleigh numbers of the problem as a function of Newton's coefficient α quantifying the intensity of heat losses through the walls.

The article is organized as follows. We first introduce the reaction–diffusion–convection model at the basis of our analysis. We next present the reaction–diffusion base state profiles for concentration and temperature as well as the way the linear stability analysis is performed numerically. We next investigate the stability changes due to heat losses for different values of parameters of the problem before concluding.

2. Model

Our system is a two-dimensional Hele-Shaw cell of size L_x x L_y oriented vertically in the gravity field (Fig. 1). The cell is initially filled with reactants and autocatalytic fronts are initiated both at the top and bottom of the cell. The products in concentration $c=c_1$ invade the reactants where $c=c_0$ in a traveling front due to the coupling between diffusion and an autocatalytic and exothermic kinetics $f(c)$ of third order. A difference in density is able to destabilize the fronts that deforms into fingers over time. The dimensional equations describing the evolution of the system are [6]

$$\underline{\nabla}\cdot\underline{u} = 0, \tag{1}$$

$$\underline{\nabla}p = -\frac{\mu}{\kappa}\underline{u} + \rho(c,T)\underline{g}, \tag{2}$$

$$\frac{\partial c}{\partial t} + \underline{u}.\underline{\nabla}c = D_c\nabla^2 c - f(c), \tag{3}$$

$$\frac{\partial T}{\partial t} + \underline{u}.\nabla T = D_T\nabla^2 T - \frac{\Delta H}{\rho_0 C_p}f(c) - \alpha'(T-T_0). \tag{4}$$

We make the assumption that the fluid is incompressible (1) and that the velocity field $\underline{u}$ and the pressure gradient $\underline{\nabla}p$ are related by Darcy's law (2), provided the gap width h of the Hele-Shaw cell is thin enough to consider the system as a two-dimensional and the permeability κ as equal to $h^2/12$. Conditions for such approximation to hold have been discussed in details by Martin et al. [13,40].

The evolution of the concentration c of the product and of the temperature T is given by reaction–diffusion–convection (RDC) Eqs. (3) and (4). ρ_0 and T_0 are the initial reactant solution density and temperature respectively. The reaction kinetics is chosen as $f(c)=kc^2(c-1)$ where k is the reaction kinetic constant. We assume that the density changes due to temperature or concentration changes are small enough so that the viscosity μ, the kinetic constant k, the molecular diffusion coefficient D_c, the thermal

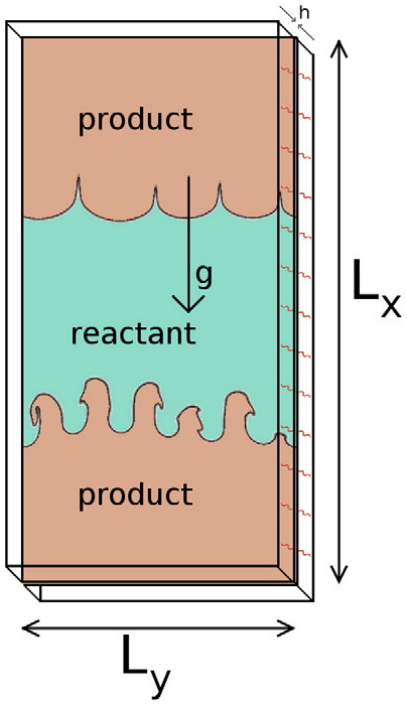

Fig. 1. Schematic of a Hele-Shaw cell oriented vertically in the gravity field. An ascending front starts from the bottom and moves upward while a descending front starts from the top and travels downward.

diffusivity D_T, the heat capacity of water C_p and the enthalpy of the autocatalytic reaction ΔH are considered as constant. Finally α' is Newton's coefficient quantifying the intensity of heat losses out of the system.

As we work with diluted solutions and have therefore only a small temperature jump across the front, the density is supposed to vary linearly with the concentration and the temperature. We write thus

$$\rho = \rho_0 + \Delta\rho_s + \Delta\rho_T. \tag{5}$$

The following characteristic time of reaction $\tau = (k\Delta c^2)^{-1}$, length $L_h = \sqrt{\tau D_c}$ and speed $U = \sqrt{\frac{D_c}{\tau}}$ are used to nondimensionalize the system of equations. The concentration $(c - c_o)$ and temperature $(T - T_o)$ are normalized by their jump across the front $\Delta c = c_1 - c_0$ and $\Delta T = T_1 - T_0 = |\Delta H|\Delta c/\rho_0 C_p$ with c_1 and T_1 the concentration and temperature of products after the reaction. The hydrostatic pressure gradient $\rho_0 \underline{g}$ is incorporated in the pressure term which is next normalized by $\frac{\mu U}{\kappa}$. We introduce the Lewis number $Le = D_T/D_c$ which is the ratio between heat and mass diffusivities. Finally, defining $\alpha = \alpha'\tau$, we obtain the following dimensionless equations

$$\underline{\nabla}\cdot\underline{u} = 0, \tag{6}$$

$$\underline{\nabla} p = -\underline{u} + (R_c c + R_T T)\underline{1}_x, \tag{7}$$

$$\frac{\partial c}{\partial t} + \underline{u}\cdot\underline{\nabla} c = \nabla^2 c - c^2(c-1), \tag{8}$$

$$\frac{\partial T}{\partial t} + \underline{u}\cdot\underline{\nabla} T = Le\nabla^2 T - c^2(c-1) - \alpha T, \tag{9}$$

with the Rayleigh numbers

$$R_T = \frac{ig\kappa\Delta\rho_s}{\mu U}, R_c = \frac{ig\kappa\Delta\rho_T}{\mu U} \tag{10}$$

The Rayleigh numbers are defined to be positive if the front is unstable. The parameter $i = \pm 1$ is therefore introduced in order to keep the same definition for R_c and R_T for both ascending and descending fronts and to be able to change in effect the direction of propagation with regard to gravity. Explicitly, we consider here descending fronts moving along $\underline{1}_x$ pointing in the same direction as gravity when $i = +1$. On the contrary, taking $i = -1$, we model ascending fronts moving in the direction opposite to $\underline{1}_x$ and to gravity [41].

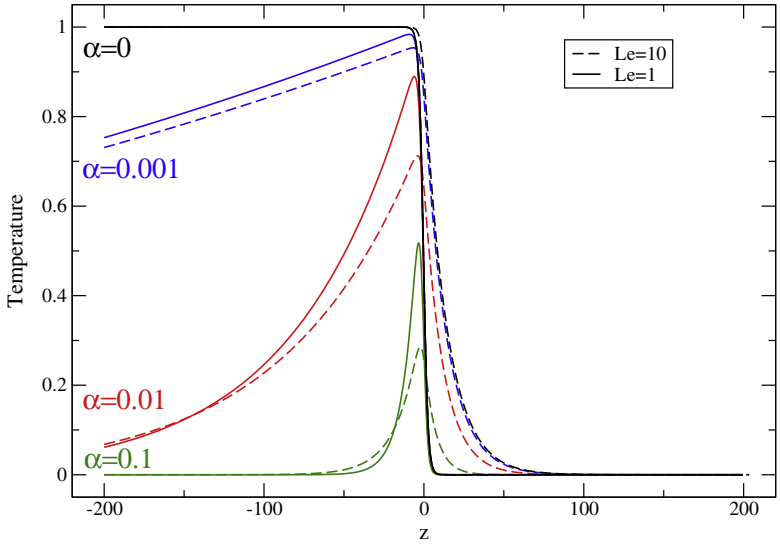

Fig. 2. Reaction–diffusion base state temperature profiles for $Le = 1$, 10 and different values of α.

3. Concentration and temperature profiles

The 1D base state reaction–diffusion concentration profile $c_o(x, t)$, solution of Eq. (8) with $\underline{u} = 0$ is given by the analytical solution [2]:

$$c_o(x,t) = \frac{1}{1 + e^{-\sqrt{1/2}(x \pm vt)}} \tag{11}$$

where the sign + and − correspond to the ascending and descending front respectively and the front speed $v = \sqrt{2}/2$. If $Le = 1$ and $\alpha = 0$, the evolution equation for the temperature (9) equals that for the concentration (8) and hence $T_o(x, t) = c_o(x, t)$. However, for other values of Le and α, the base state profile T_o cannot be obtained analytically and must be computed by numerical integration of the coupled reaction–diffusion equations (Eqs. (8) and (9)). Fig. 2 shows temperature profiles in a reference frame $z = x - vt$ for various values of Le and α. When $\alpha = 0$, we get a front between the ambiant dimensionless temperature $T = 0$ and the adiabatic product temperature $T = 1$. The larger the Lewis number, the more spread out the front. In presence of heat losses $\alpha \neq 0$, the temperature profile becomes a pulse with the largest temperature obtained inside the front in the reaction zone while the products behind the front are cooled off because of the heat losses through the glass plates. The larger α the more intense the heat losses and the smaller the maximum temperature in the system (Fig. 3). Increasing Le for a fixed value of α also spreads the temperature profile and hence, decreases the maximum temperature.

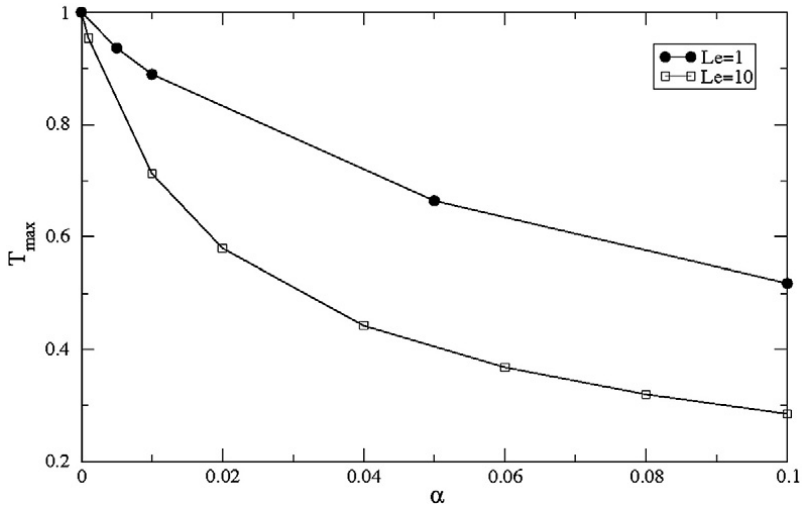

Fig. 3. Maximum temperature reached in the reaction–diffusion profile as a function of α for $Le = 1$ and $Le = 10$.

4. Linear stability analysis

In order to analyze how changes in Le and in α influence the stability of fronts with regard to buoyancy-driven instabilities for both ascending or descending fronts of cooperative or antagonist cases, we consider a setup like shown on Fig. 1. The system is thus a Hele-Shaw with conducting walls filled with reactants ($c=0, T=0$) and oriented vertically in the gravity field. Autocatalytic fronts are initiated both at the top and the bottom of the cell so that we can follow both descending and ascending fronts. We seek to understand how density differences across such fronts can destabilize them with regard to buoyancy-driven instabilities. To do so, we will perform a linear stability analysis of the base state profiles $c_o(x,t)$ and $T_o(x,t)$ with regard to transverse perturbations. Explicitly, we follow the procedure detailed in Ref.[32] to obtain dispersion curves $\sigma=\sigma(k)$ i.e. the growth rate σ of the perturbations as a function of their wavenumber k for given values of the parameters α, R_c and R_T. The system will feature a hydrodynamic instability i.e. the front will develop a transverse modulation like shown on Fig. 1 as soon as $\sigma>0$ for any given wavenumber k. Throughout the article, we next fix $Le=10$, a typical value observed for the chlorite–tetrathionate reaction [5,24,25]. This ratio is small in comparison with typical Lewis numbers for other chemical species because the autocatalytic species is here the proton which, in diluted aqueous solutions, diffuses fast through the hydrogen bond network of water molecules. In IAA reaction, where $Le\sim 50-70$ [42], thermal effects are correspondingly much weaker [28].

5. Results

A synthetic way to visualize the global effect of heat losses on the stability of autocatalytic fronts is to delineate the stability regions in the parameter space spanned by R_c and R_T (Fig. 4). To appreciate changes of stability when α is varied, it is necessary to first recall the situation in absence of heat losses.

5.1. Isolated systems $\alpha=0$

To fix ideas, we recall that, in isolated systems ($\alpha=0$) and considering solutal and thermal effects separately, the front is genuinely buoyantly unstable when $R_c>0$ corresponding to a solute–denser solution on top of a less dense one or when $R_T>0$ for which a hot solution is put below a colder one. The top right quadrant where R_c and R_T are both positive corresponds therefore to ascending cooperative fronts for which the denser reactants at room temperature overlie less dense and hotter products. This quadrant is always unstable [21] whatever the value of Le and of α. The reverse situation $R_c<0$, $R_T<0$ stands for descending cooperative fronts which, for isolated systems and $Le=1$, are stable because hot, less dense products are then on top of the colder denser reactants. If $Le\neq 1$, D'Hernoncourt et al. have shown that a new instability related to the coupling of the reaction with differential diffusion effects between heat and mass can destabilize such descending fronts [6,20,21]. In that case, the larger $Le>1$, the larger the instability zone.

For antagonist fronts, solutal and thermal effects are competing and for $Le=1$, the system is always unstable provided the destabilizing component has the largest Rayleigh number. For example, for ascending cooperative fronts ($R_c<0$, $R_T>0$), the front deforms if the products are hot enough (in effect $R_T>|R_c|$) to obtain a globally unstable density stratification. Hence for $Le=1$ the whole plane region to the right of the line $R_T=-R_c$ is unstable. For $Le>1$, the instability domain is much larger because of differential diffusion phenomena classically active when heat and mass effects compete [6,19,21].

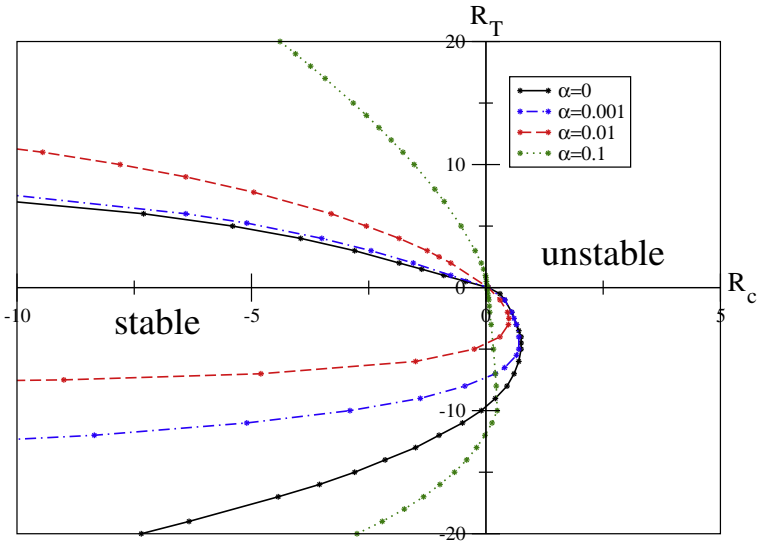

Fig. 4. Stability regions in the parameter space (R_c, R_T) for different α and Le = 10. The left side of the curves corresponds to stable fronts while the unstable ones are at their right.

5.2. Open systems $\alpha \neq 0$

To see how heat losses modify the above stability regions, we have computed dispersion curves for couples of Rayleigh numbers at fixed values of α (Fig. 4). For a fixed R_T, we look for the threshold value of R_c (with a precision between $dR_c = 0.01 - 0.05$) above which the growth rate becomes positive ($\sigma \geq 0.001$) for any given wavenumber. This allows to delineate the region of parameter space where the system remains stable (Fig. 4). The left side of the curves is here the region of stable fronts while the fronts with larger R_c are unstable. Globally, we note that for ascending fronts ($R_T > 0$), the cooperative ones ($R_c > 0$) remain always unstable whatever the intensity of the heat losses while the antagonist ones ($R_c < 0$) have a larger stability domain when α increases. For descending fronts however ($R_T < 0$), the influence of heat losses is less trivial as we observe a destabilization for intermediate values of α and an extension again of the stable zone for larger values of α. To gain more insight into this global perception, let us compute density profiles. Note that for isothermal systems ($\alpha = \infty$), the instability region is simply the half plane $R_c > 0$.

5.3. Density profiles

The Rayleigh–Taylor instability develops when a denser solution overlies a less dense one in the gravity field. It is therefore instructive to plot density profiles to analyze for which values of parameters such as adverse density stratification can develop either globally or locally. Fig. 5 shows density profiles $\rho(z) = i(R_c c + R_T T)$ (first column) and related dispersion curves (second column) for each quadrant of Fig. 4 for $|R_c| = 5$ and $|R_T| = 10$. We recall that $\mathrm{i} = -1$ for ascending fronts traveling against the direction of gravity while $\mathrm{i} = +1$ for descending ones. In the density profiles, the products ($c = 1$) are always at the left of the figure. The middle of the concentration front ($c = 0.5$) is located at $z = 0$, while the reactants ($c = 0$) are at the right of the graph. As $c = 0$ and $T = 0$ in the reactant solution far ahead of the front, the related density $\rho_r = 0$. Far behind the front, the products where $c = 1$ and $T = 1$ have a density $\rho_p = i(R_c + R_T)$ at $z = -\infty$ in absence of heat losses ($\alpha = 0$). When $\alpha > 0$, the product temperature decreases with the distance to the front and, at $z = -\infty$, $T \to 0$, leading to a density $\rho_p \to iR_c$. Positive values of R_c or R_T mean a globally unstable stratification of density. For each picture we are showing the results for various intensities of α and also for an isothermal system equivalent to $\alpha = \infty$. Let us now analyze the influence of heat losses in each quadrant.

5.4. First quadrant: $R_c > 0$, $R_T > 0$

$R_c > 0$, $R_T > 0$, and $i = -1$ corresponds to an unstable stratification of ascending cooperative fronts with solute–denser and colder reactants at a density $\rho_r = 0$ on top of solute less dense and hotter products with density $\rho = -R_c - R_T$. This is the case of ascending IAA fronts for instance. Fig. 5.1a shows the related density profiles for $R_c = 5$, $R_T = 10$ and different heat losses. If $\alpha = 0$, the thermal and solutal effects add up to generate a density front whereby the denser reactants overlie the less dense products. A Rayleigh–Taylor instability is observed leading to fingers already well studied both experimentally [12–14,16] and numerically [15].

If the walls are conductive, the thermal destabilizing effect is dampened and if $\alpha \to \infty$, the RT instability is weakened to the sole solutal component which is yet still destabilizing. This is confirmed by the dispersion curves (Fig. 5.1b) which show that growth rates remain positive whatever the value of α confirming that the solutal destabilizing component remains sufficient in any case to destabilize the front. As the maximum value of temperature decreases non monotonically with α (see Fig. 3), dispersion curves also vary in a non monotonic way between the most unstable dispersion curve for $\alpha = 0$ toward the pure solutal case $\alpha = \infty$.

5.5. Second quadrant: $R_c < 0$, $R_T > 0$

The second quadrant where $R_c < 0$, $R_T > 0$ features a stable solutal density stratification (R_c negative) yet an unstable thermal one (R_T positive) which corresponds to ascending antagonist fronts whereby solute-less dense reactants at room temperature are located above solute–denser yet hotter products. If $Le = 1$, thermal effects are winning above the line $R_T = -R_c$ i.e. their amplitude is then larger than that of the solutal effects such that the overall density gradient is positive upwards (i.e. toward positive x) and thus unstable.

D'Hernoncourt et al. [6,21] have shown that, for $\alpha = 0$, the instability zone is largely increased when Le is increased above 1 (Fig. 4) because faster diffusion of heat produces a non-monotonic density profile with locally sharper gradients (Fig. 5.2a). Differential diffusion effects also contribute to increase instability. As the thermal component is here destabilizing, heat losses actually weaken this destabilizing component and we observe a decrease in the growth rate and in the band of unstable modes when α is increased (Fig. 5.2b). Eventually, in isothermal systems ($\alpha = \infty$), the system is stable with all modes having negative growth rates because the sole remaining solutal component to density is stabilizing ($R_c < 0$).

A comparison of Fig. 5.1 and 5.2 shows that the density jump is the same between $\rho_r = 0$ and $\rho_p = -5$ when $R_c = 5$, $\alpha = \infty$ in Fig. 5.1 or when $R_c = -5$, $R_T = 10$, $\alpha = 0$ in Fig. 5.2. Yet the intensity of σ is smaller and the band of unstable wavenumbers smaller too in quadrant 2. This is related to the fact that, in the former case, the density jump is related solely to the solutal effect while in the second case it is the thermal component which is destabilizing. As $Le > 1$, the temperature profile is more spread out than the concentration one and hence the density gradient is smaller which explains why the system is less unstable.

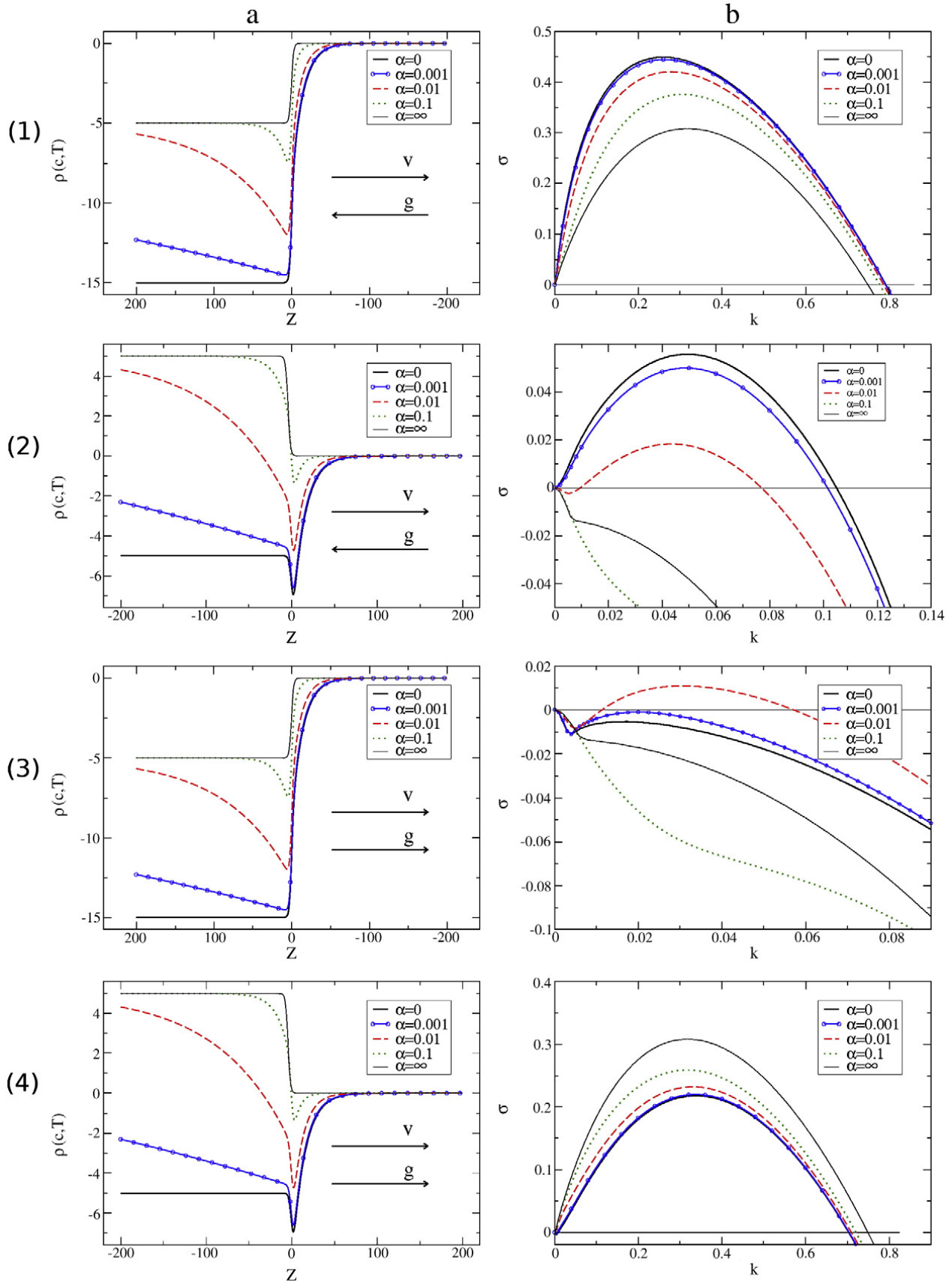

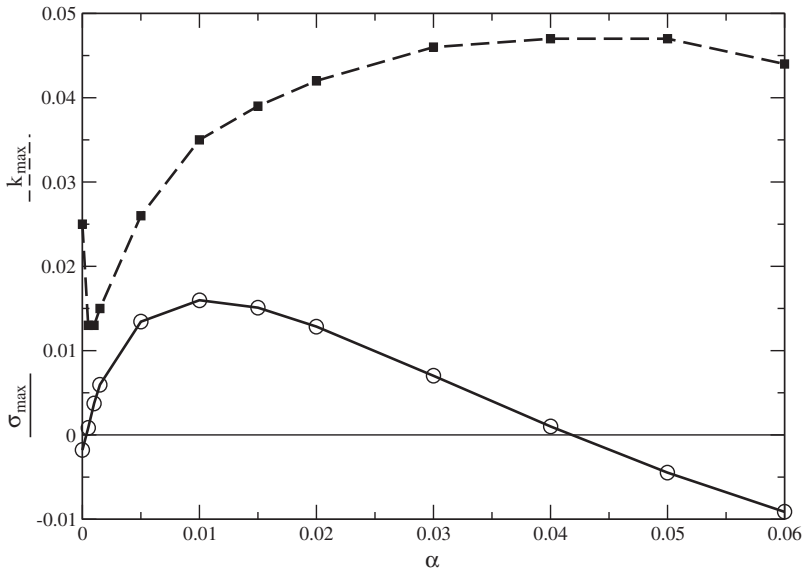

Fig. 6. Most unstable value of the growth rate σ_{max} and of the wavenumber k_{max} as a function of α for $R_c=-1$, $R_T=-10$ and $Le=10$ i.e. in quadrant 3.

5.6. Third quadrant: $R_c<0$, $R_T<0$

The third quadrant is the most interesting quadrant. The Rayleigh numbers are both negative which means that the solutal and thermal effects on density are both stabilizing. This applies to cooperative descending fronts featuring solute-less dense and hotter products invading downwards solute–denser and colder reactants. Intuitively, one would expect stability in this quadrant, yet a linear stability analysis of the problem in insulated systems has already pointed out to the possibility of destabilization [20] by coupling of the reaction with double diffusive effects when $Le>1$.

Heat losses have a non-trivial effect on this instability as can be appreciated on Figs. 4 and 6 which show that the instability domain is changing non-monotonically with α. For small α, the fronts are further destabilized by heat losses as the instability region is larger (Fig. 4). This can be understood by inspecting the related density profiles on Fig. 5.3a. For $\alpha=0$, we have a density increasing monotonically along x featuring thus a stable stratification of less dense over dense. Instability is in that case related to double diffusive effects and to a subtle coupling between reaction and convection [20]. However, once heat losses become operative, the products are cooled down which leads locally to a Rayleigh–Taylor unstable stratification of denser cooled products behind the front over hotter and thus less dense products inside the front [32]. This effect induces an increase of the instability domain (Fig. 4) and of σ_{max} (Fig. 6) for increasing moderate α leading to sharper negative gradients behind the front as seen when comparing the density profiles for $\alpha=0$, 0.001 and 0.01 on Fig. 5.3a.

Fig. 5.3b shows that, for $\alpha=0$ and 0.001, the front is stable for $R_c=-5$ and $R_T=-10$. However, increasing α to 0.01 gives a band of unstable modes. Note that the perturbations of small k have negative values of $\sigma<0$. Consequently, the fingers of such fronts will not coalesce into one big finger as when the band of unstable modes extends down to $k=0$ but will feature a well-defined constant wavelength [32,33]. In the nonlinear regime, the presence of a pulse of heat inside the front induces enhanced tip splittings [32,33], a velocity field arranged in a quadrupole rather than in a dipole [16,33] as well as hot spots [29].

Eventually however, for large heat losses, the front is stable again because, if the thermal effects are canceled, both coupling of reaction with differential diffusion effects between heat and mass as well as the local unstable Rayleigh–Taylor mechanism due to local heating of products inside the front are suppressed. Fig. 6 summarizes this non-monotonic influence of α on stability of descending cooperative fronts showing that the maximum growth rate σ_{max} is obtained for $\alpha\simeq0.01$. For larger heat losses, σ_{max} decreases and the system is stable again for $\alpha>0.041$.

5.7. Fourth quadrant: $R_c>0$, $R_T<0$

If $R_c>0$, $R_T<0$, we have the reverse case of the second quadrant i.e. we consider descending cooperative fronts in which hot but solute–denser products invade downwards colder but solute less dense reactants. Solutal effects are destabilizing ($R_c>0$) while thermal ones are stabilizing ($R_T<0$). As in quadrant 2, the density profile is globally RT unstable for $Le=1$ above the line $R_T=-R_c$. However, the instability zone is much larger because of double diffusive effects [5]. In this case, heat losses lead to a decrease of the stabilizing component such that in the limit of $\alpha=\infty$, the whole $R_c>0$ half plane is unstable.

Fig. 5. Density profiles (left) and dispersion curves (right) for $Le=10$, $\alpha=0$, 0.001, 0.01 and 0.1 for the four quadrants: (1) $R_c=5$, $R_T=10$, (2) $R_c=-5$, $R_T=10$, (3) $R_c=-5$, $R_T=-10$, (4) $R_c=5$, $R_T=-10$. (1–2) represent ascending cooperative (1) and antagonist (2) fronts respectively with the fronts traveling toward negative x while gravity points toward positive x. (3–4) represent descending cooperative (3) and antagonist (4) fronts respectively with the fronts traveling toward positive x aligned with gravity.

6. Conclusion

Heat losses have a profound influence on the stability of autocatalytic chemical fronts with regard to buoyancy-driven instabilities. Whether the reaction is of cooperative or antagonist nature or whether the front is ascending or descending in the gravity field, heat losses modify the dispersion curves of the problem. In the limit of the isothermal system (Newton's coefficient $\alpha = \infty$), the whole half plane $R_c > 0$ is unstable. For intermediate values of α, the influence of heat losses has various trends. For ascending cooperative fronts, heat losses stabilize the system because they decrease the destabilizing thermal contribution to the density profile. For descending cooperative fronts, the influence of heat losses is more subtle. Indeed, for intermediate heat losses, the density profile features an unstable stratification of cooled products above hotter products inside the reaction zone which is increasing the instability domain with regard to the insulated system. For large heat losses however, the contribution of heat to possible differential diffusion effects is vanishing and we recover stable isothermal fronts. For antagonist systems in which solutal and thermal effects on density compete, the influence of heat losses is again non-monotonic for descending fronts while they stabilize ascending fronts for which the thermal contribution is destabilizing.

Let us note that our results have been obtained with a 2D model using Darcy's law. As it is known that 3D effects may occur depending on the value of the gap width [13,40], it would be of interest in future studies to take such a third dimension into account as indeed the gap also influences the intensity of heat losses.

The present article has focused on the influence of heat losses in Hele-Shaw cells oriented vertically in the gravity field such that gravity points perpendicularly to the front. Recently, experiments and theoretical works have also started analyzing dynamics of exothermic fronts in horizontal systems [43–45]. Thermal effects are particularly important in these dynamics too as hot zones rise on top of colder ones. In antagonist systems as for the CT reaction for instance, competition between solutal and thermal contributions to density can even lead to oscillatory dynamics when $Le > 1$ [44]. These theoretical studies have been performed assuming insulated reactors. In view of the important influence of heat losses shown here, it will be of interest in the future to analyze stability and dynamics of exothermic fronts in horizontal Hele-Shaw cells taking such heat losses into account as well.

Acknowledgment

This article is dedicated to Professor C. Christov. A.D. thanks him for nice memories and fruitful discussions all over the years. T. Gérard acknowledges financial support from FRIA.

References

[1] V. Mendez, S. Fedotov, W. Horsthemke, Reaction–Transport Systems, Springer Verlag, 2010.
[2] A. Saul, K. Showalter, Propagating reaction–diffusion fronts, in: R. Fields, M. Burger (Eds.), Oscillations and Travelling Waves in Chemical Systems, 1985.
[3] I.R. Epstein, J.A. Pojman, An Introduction to Nonlinear Chemical Dynamics, Oxford University, Oxford, 1998.
[4] J.A. Pojman, I.R. Epstein, J. Phys. Chem. 94 (1990) 4966.
[5] S. Kalliadasis, J. Yang, A. De Wit, Phys. Fluids 16 (2004) 1395.
[6] J. D'Hernoncourt, A. Zebib, A. De Wit, Chaos 17 (2007) 013109.
[7] J.A. Pojman, I.R. Epstein, T.J. McManus, K. Showalter, J. Phys. Chem. 95 (1991) 1299.
[8] J. Masere, D.A. Vasquez, B.F. Edwards, J.W. Wilder, K. Showalter, J. Phys. Chem. 98 (1994) 6505.
[9] J. Huang, B.F. Edwards, Phys. Rev. E 54 (1996) 2620.
[10] M. Carey, S.W. Morris, P. Kolodner, Phys. Rev. E 53 (1996) 6012.
[11] A. De Wit, Phys. Rev. Lett. 87 (2001) 054502.
[12] M. Böckmann, S.C. Müller, Phys. Rev. Lett. 85 (2000) 2506.
[13] J. Martin, N. Rakotomalala, D. Salin, M. Böckmann, Phys. Rev. E 65 (2002) 051605.
[14] M. Böckmann, S.C. Müller, Phys. Rev. E 70 (2004) 046302.
[15] A. De Wit, Phys. Fluids 16 (2004) 163.
[16] L. Šebestíková, J. D'Hernoncourt, M.J.B. Hauser, S.C. Müller, A. De Wit, Phys. Rev. E 75 (2007) 026309.
[17] M.C. Rogers, M.D. Mantle, A.J. Sederman, S.W. Morris, Phys. Rev. E 77 (2008) 026105.
[18] M.C. Rogers, A. Zebib, S.W. Morris, Phys. Rev. E 82 (2010) 066307.
[19] J.S. Turner, Buoyancy Effects in Fluids, Cambridge University Press, Cambridge, England, 1973.
[20] J. D'Hernoncourt, A. Zebib, A. De Wit, Phys. Rev. Lett. 96 (2006) 154501.
[21] J. D'Hernoncourt, A. De Wit, A. Zebib, J. Fluid Mech. 576 (2007) 445.
[22] J.A. Pojman, I. Nagy, I.R. Epstein, J. Phys. Chem. 95 (1991) 1306.
[23] T. Bánsági Jr., D. Horváth, Á. Tóth, Phys. Rev. E 68 (2003) 026303.
[24] T. Bánsági Jr., D. Horváth, Á. Tóth, J. Yang, S. Kalliadasis, A. De Wit, Phys. Rev. E 68 (2003) 055301.
[25] T. Bánsági Jr., D. Horváth, Á. Tóth, Chem. Phys. Lett. 384 (2004) 153.
[26] T. Tóth, D. Horváth, A. Tóth, Chem. Phys. Lett. 442 (2007) 289.
[27] G. Casado, L. Tofaletti, D. Müller, A. D'Onofrio, J. Chem. Phys. 126 (2007) 114502.
[28] J. Martin, N. Rakotomalala, L. Talon, D. Salin, Phys. Rev. E 80 (2009) 055101.
[29] P. Grosfils, F. Dubois, C. Yourassowsky, A. De Wit, Phys. Rev. E 79 (2009) 017301.
[30] V.V. Zhivonitko, I.V. Koptyug, R.Z. Sagdeev, J. Phys. Chem. Lett. 111 (2007) 4122.
[31] D. Horváth, T. Bánsági Jr., A. Tóth, J. Chem. Phys. 117 (2002) 4399.
[32] J. D'Hernoncourt, S. Kalliadasis, A. De Wit, J. Chem. Phys. 123 (2005) 234503.
[33] J. D'Hernoncourt, A. De Wit, Physica D 239 (2010) 819.
[34] O. Manickam, G.M. Homsy, Phys. Fluids 5 (1993) 1356.
[35] F.J. Hickernell, Y.C. Yortsos, Stud. Appl. Math. 74 (1986) 93.
[36] E.D. Chikhliwala, A.B. Huang, Y.C. Yortsos, Transp. Porous Media 3 (1988) 257.
[37] D. Loggia, N. Rakotomalala, D. Salin, Y.C. Yortsos, Europhysics Lett. 22 (1995) 633.
[38] C. Almarcha, P.M.J. Trevelyan, P. Grosfils, A. De Wit, Phys. Rev. Lett. 104 (2010) 044501.
[39] C. Almarcha, P.M.J. Trevelyan, L.A. Riolfo, A. Zalts, C. El Hasi, A. D'Onofrio, A. De Wit, J. Phys. Chem. Lett. 1 (2010) 752.

[40] J. Martin, N. Rakotomalala, D. Salin, Phys. Fluids 14 (2002) 902.
[41] Alternatively, one can fix $i = +1$ throughout and let $\underline{1}_x$ point downwards for descending fronts and upwards for ascending ones as done in ref. [6].
[42] J.W. Wilder, B.F. Edwards, D.A. Vasquez, Phys. Rev. A 45 (1992) 2320.
[43] L. Rongy, A. De Wit, J. Chem. Phys. 131 (2009) 184701.
[44] L. Rongy, G. Schuszter, Z. Sinkó, T. Tóth, D. Horváth, A. Tóth, A. De Wit, Chaos 19 (2009) 023110.
[45] I. Bou Malham, N. Jarrige, J. Martin, N. Rakotomalala, L. Talon, D. Salin, J. Chem. Phys. 133 (2010) 244505.